Graduated dark energy: Observational hints of a spontaneous sign switch in the cosmological constant

Özgür Akarsu,[1,*] John D. Barrow,[2,†] Luis A. Escamilla,[3,‡] and J. Alberto Vazquez[3,§]

[1]*Department of Physics, Istanbul Technical University, Maslak 34469 Istanbul, Turkey*
[2]*DAMTP, Centre for Mathematical Sciences, University of Cambridge, Wilberforce Road, Cambridge CB3 0WA, United Kingdom*
[3]*Instituto de Ciencias Físicas, Universidad Nacional Autónoma de México, Cuernavaca, Morelos, 62210, México*

(Received 19 December 2019; accepted 5 March 2020; published 25 March 2020)

We study the cosmological constant (Λ) in the standard Λ cold dark matter model by introducing the *graduated dark energy* (gDE) characterized by a minimal dynamical deviation from the null inertial mass density of the Λ in the form $\rho_{\rm inert} \propto \rho^{\lambda} < 0$ with $\lambda < 1$ being a ratio of two odd integers, for which its energy density ρ dynamically takes negative values in the finite past. For large negative values of λ, it creates a phenomenological model described by a smooth function that approximately describes the Λ spontaneously switching sign in the late Universe to become positive today. We confront the model with the latest combined observational datasets of Planck + baryon acoustic oscillations + supernova + H. It is striking that the data predict bimodal posterior probability distributions for the parameters of the model along with large negative λ values; the new maximum significantly excludes the Λ, and the old maximum contains the Λ. The improvement in the goodness of fit for the Λ reaches highly significant levels, $\Delta\chi^2_{\rm min} = 6.4$, for the new maxima, while it remains at insignificant levels, $\Delta\chi^2_{\rm min} \lesssim 0.02$, for the old maxima. We show that, in contrast to the old maxima, which do not distinguish from the Λ, the new maxima agree with the model-independent H_0 measurements, high-precision Ly-α data, and model-independent Omh^2 diagnostic estimates. Our results provide strong hints of a spontaneous sign switch in the cosmological constant and lead us to conjecture that the Universe has transitioned from anti-de Sitter vacua to de Sitter vacua, at a redshift $z \approx 2.32$, and triggered the late-time acceleration, and suggests looking for such mechanisms in string theory constructions.

DOI: 10.1103/PhysRevD.101.063528

I. INTRODUCTION

The standard Lambda cold dark matter (ΛCDM) model, relying on the inflationary paradigm [1–4], has proven so far to be the most successful cosmological model that accounts for the dynamics and the large-scale structure of the Universe. It is in excellent agreement with a wide variety of the currently available data [5–9]. Nevertheless, in addition to its long-standing profound theoretical issues relating to the Λ (or conventional vacuum energy) [10–13], it has recently begun to suffer from persistent tensions of various degrees of significance between some existing datasets (see, e.g., Refs. [14–18] for further reading). Such tensions are of great importance as detection of even small deviations from the standard ΛCDM model with high significance could have substantial implications on our understanding of the fundamental theories of physics underpinning it.

One of the most intriguing tensions reported so far is the significant deficiency in the Hubble constant H_0 value predicted by the cosmic microwave background (CMB) Planck data [6,9] using the base ΛCDM model when compared with the values by direct model-independent local measurements [19–22]. The fact that it worsens for the simplest minimally coupled single-field quintessence models and is only partially relieved by phantom models (or quintom models) aggravates this tension as it suggests the elimination of these standard dark energy (DE) models [23–25] (see also Ref. [26] for further references). Surprisingly, the situation changes if the DE energy density is not restricted to be strictly positive. It has been reported that a number of persistent low-redshift tensions, including the H_0 tension, may be alleviated by a dynamical DE whose energy density can assume negative values or vanish at a finite redshift [26–37].

The possible need for DE whose energy density can assume negative values was previously emphasized by the

*akarsuo@itu.edu.tr
†J.D.Barrow@damtp.cam.ac.uk
‡luis.escamilla@icf.unam.mx
§javazquez@icf.unam.mx

observation that, when the base ΛCDM model is considered, the Ly-α forest measurement of the baryon acoustic oscillations (BAOs) by the BOSS Collaboration prefers a smaller value of the dust density parameter than is preferred by the CMB data [35]. They reported a clear detection of DE consistent with $\Lambda > 0$ for $z < 1$, but with a preference for a DE assuming negative energy density values for $z > 1.6$, and argued that the Ly-α data from $z \approx 2.34$ can fit a nonmonotonic evolution of $H(z)$, i.e., of the total energy density $\rho_{\rm tot}(z)$—assuming general relativity—which is difficult to achieve in any model with non-negative DE density [36]. In another study [37], in line with this, it was argued that the Ly-α data can be accommodated by a physically motivated modified gravity model that alters $H(z)$ itself, and also that a further tension relevant to the Ly-α data can be alleviated in models in which Λ is dynamically screened, implying an effective DE passing below zero and concurrently exhibiting a pole in its equation of state (EoS), at $z \sim 2.4$. DE models—either as a physical source or an effective source arising from a modified theory of gravity—assume negative energy density values have not been paid much attention so far (for reviews on DE and modified theories of gravity, see Refs. [38–44]). However, such scenarios are in fact familiar from an effective source (say, DE) defined by the collection of all modifications to the usual Einstein field equations in scalar-tensor theories, namely, when the cosmological gravitational coupling strength gets weaker with increasing redshift [45,46]. A range of other examples of effective sources crossing below zero also exists, including theories in which Λ relaxes from a large initial value via an adjustment mechanism [47,48], in cosmological models based on Gauss-Bonnet gravity [49], in braneworld models [50,51], in loop quantum cosmology [52,53], in higher-dimensional cosmologies that accommodate dynamical reduction of the internal space [54–57], and generalizations of the form of the matter Lagrangian in a nonlinear way [58–60].

It is possible to seek such scenarios by following a minimalist approach, namely, starting with the minimal extensions to the standard ΛCDM model. The most natural one to consider is the addition of positive spatial curvature, e.g., that of the Friedmann-Robertson-Walker (FRW) spacetime which imitates a negative energy density source with an EoS parameter equal to $-1/3$. It is easy to check that, however, to screen Λ at, e.g., $z \sim 2.4$ for $\Omega_{\Lambda,0} \sim 0.7$, its density parameter today is required to be $\Omega_{k,0} \sim -0.06$, which contradicts the inflationary paradigm and is indeed not allowed, e.g., by the joint results of the recent Planck release [9] suggesting spatial flatness to a 1σ accuracy of 0.2%. If we stay loyal to the inflationary paradigm and then suppose flat space, the simplest source that can realize such a behavior can be obtained by promoting the null *inertial mass density* [61,62] of the vacuum energy ($\rho_{\rm inert} = 0$) to a negative constant, $\rho_{\rm inert} = \text{const} < 0$. The source $\rho_{\rm inert} = \text{const}$ has recently been of interest to many as it mimics Λ today while leading the Universe to exhibit a future singularity dubbed the little sibling of the big rip for $\rho_{\rm inert} = \text{const} < 0$ and a finite future bounce for $\rho_{\rm inert} = \text{const} > 0$ [63,64]. However, in the light of the observational analyses carried out in this paper, $\rho_{\rm inert} = \text{const} < 0$ provides us with neither a superior DE model with respect to the Λ nor an improvement regarding the tensions of interest to us. For instance, the observational data suggest that its energy density changes sign at a redshift larger than 65 (i.e., when it is already negligible) and it is indistinguishable from Λ today ($z \sim 0$), so clearly it cannot have consequences for the tensions with which we are concerned. The simplest next step may be to consider the minimum *dynamical* deviation from the null inertial mass density, viz., in the form $\rho_{\rm inert} \propto \rho^{\lambda} < 0$ with λ being a real constant. The exponent λ here will provide us with a more featured evolution of the energy density passing below zero at high redshifts. Importantly, for arbitrarily large negative values of λ, it resembles a step function in redshift describing a *spontaneously sign-switching cosmological constant* at a certain redshift. Accordingly, it can also be viewed as a phenomenological model described by a smooth function for approximately describing a vacuum energy that switches sign at a certain redshift and becomes positive just recently in the late Universe and triggers the acceleration. A source having this form (but considering $\rho_{\rm inert} \propto \rho^{\lambda} > 0$) was first suggested in Ref. [65] (see also Refs. [66,67]) for introducing an intermediate inflationary scenario named *graduated inflation*. It was physically motivated by the form of bulk viscous stresses in FRW models and their quantum counterparts when the bulk viscosity is proportional to a power of the density.

Accordingly, we shall call this source *graduated dark energy* (gDE) as in this paper we study the present-day acceleration of the Universe. In fact, more recently, it has also been considered as a DE (e.g., Refs. [68–71]). However, all these works focus on the future singularities and the asymptotic dynamics of the Universe by retaining the positivity of the energy density (the cases for the negative energy density are discussed only superficially). In contrast, here, we focus on its dynamics around the present time and utilize its sign-switching energy-density feature to address the tensions that arise within ΛCDM model when the data from the late Universe are considered.

Such scenarios, in particular, the sign-switching cosmological constant that arises as a limiting case of the gDE, can be extremely appealing from a string theoretic perspective. Constructing metastable de Sitter (dS) vacua (provided by $\Lambda > 0$) has notoriously been a challenging task in string theory and, so far, has not been concretely achieved [72–81]. This has led many to suggest that string theory might not have any dS vacua at all [82–87]. This would obviously have immense implications in cosmology and/or theoretical physics, as it seems to

imply an inconsistency between string theory and the Universe we live in [88–98]. In contrast, an anti-de Sitter (AdS) background (provided by $\Lambda < 0$) solution naturally arises in string theory or string theory motivated supergravities with broken/unbroken supersymmetry. Furthermore, the AdS space provides a very powerful setup to study various strongly coupled quantum field theories via the AdS/CFT correspondence [99,100]. Contrary to the case of dS, which can only arise with broken supersymmetry, there does seem to exist a large number of consistent AdS backgrounds that can be obtained from string theory. It has also recently been claimed that transition from AdS vacua to dS vacua could be realized in a noncommutative quantum field theory setup [101]. Consequently, if we could show through gDE that the observational data prefer a DE having $\rho \sim \rho_0 > 0$ (positive cosmological constant) for $z \sim 0$ (just recently) and $\rho \sim -\rho_0 < 0$ (negative cosmological constant) for $z \gg 0$ (most of the history of the Universe), which is realized at large negative λ values of gDE, and that the persistent tensions arising within the standard ΛCDM model disappear/relax, this would have far reaching implications for our understanding of the fundamental laws of physics. We will show, by means of gDE, that the observational data provide strong pointers in this direction. This leads us to conjecture that the cosmological constant has spontaneously switched sign and become positive, namely, the Universe has transitioned from AdS vacua to dS vacua, at $z \sim 2.3$, and triggered the observed late-time acceleration, and we suggest looking for such mechanisms in string theory.

II. GRADUATED DARK ENERGY

The energy-momentum tensor describing an isotropic perfect fluid can be decomposed relative to a unique four-velocity, u^μ, in the form, $T_{\mu\nu} = (\rho + p)u_\mu u_\nu + p g_{\mu\nu}$, where ρ is the relativistic energy density relative to u^μ, p is the isotropic pressure, $g_{\mu\nu}$ is the metric tensor, and $\nabla_\nu u^\mu u_\mu = 0$ and $u_\mu u^\mu = -1$. The set of equations arises from the twice-contracted Bianchi identities, which by means of Einstein field equations, $G_{\mu\nu} = -T_{\mu\nu}$, implies the conservation equations. Projecting parallel and orthogonal to u_μ, we obtain the energy and momentum conservation equations, correspondingly,

$$\dot{\rho} + \Theta\rho_{\text{inert}} = 0 \quad \text{and} \quad \mathrm{D}^\mu p + \rho_{\text{inert}}\dot{u}^\mu = 0, \tag{1}$$

where $\rho_{\text{inert}} = \rho + p$, the multiplier of the four acceleration $\dot{u}^\mu$, is the inertial mass density [61,62]. Here, D_ν is the spatial gradient (the covariant derivative operator orthogonal to u^μ) defined by $\mathrm{D}_\nu f = \nabla_\nu f + u_\mu \dot{f}$; $\Theta = \mathrm{D}^\mu u_\mu$ is the volume expansion rate, and overdots denote derivatives with respect to the comoving proper time t.

Inspired by Ref. [65], we define a type of DE model, we named *graduated dark energy*, which yields an inertial mass density exhibiting power-law dependence to its energy density as follows,

$$\rho_{\text{inert}} = \gamma\rho_0\left(\frac{\rho}{\rho_0}\right)^\lambda, \tag{2}$$

where ρ_0 is positive definite (throughout the paper, subscript 0 attached to any quantity denotes its value today) and the parameters γ and λ are real constants. This can be viewed as characterizing the minimum dynamical deviation from the null inertial mass density, viz., from the conventional vacuum energy. So that EoS parameter is $w = p/\rho = -1 + \rho_{\text{inert}}/\rho$ and reads

$$w = -1 + \gamma\left(\frac{\rho}{\rho_0}\right)^{\lambda-1}. \tag{3}$$

We note that $\gamma = 0$ corresponds to the conventional vacuum energy with $w = -1$ (leading to the ΛCDM model) and $\lambda = 1$ corresponds to the perfect fluid with constant EoS parameter $w = -1 + \gamma = \text{const}$ (leading to the wCDM model). From the continuity equation (1), this leads to $\mathrm{d}\rho + 3\gamma\rho_0(\frac{\rho}{\rho_0})^\lambda \frac{\mathrm{d}a}{a} = 0$, which is solved by

$$\rho = \rho_0[1 + 3\gamma(\lambda - 1)\ln a]^{\frac{1}{1-\lambda}}, \tag{4}$$

which satisfies

$$\rho_{\text{inert}} = \gamma\rho_0[1 + 3\gamma(\lambda - 1)\ln a]^{\frac{\lambda}{1-\lambda}}, \tag{5}$$

$$w = -1 + \frac{\gamma}{1 + 3\gamma(\lambda - 1)\ln a}. \tag{6}$$

We note that $w = -1 + \gamma$ today (when $a = 1$ or redshift $z \equiv -1 + \frac{1}{a} = 0$) and $w \approx -1$ for sufficiently large and small a, in particular, $w \to -1$ in the far future ($a \to \infty$) and in the very early Universe ($a \to 0$). Besides, provided that the parameters γ and λ are chosen appropriately, gDE can achieve transition from $\rho > 0$ to $\rho < 0$ at a certain redshift. Thus, gDE can also be viewed as a phenomenological model described by a smooth function for approximately describing the cosmological constant switches sign at a certain redshift and, for instance, becomes positive just recently in the late Universe.

The gDE (4), in fact, exhibits various types of dynamics depending on its free parameters λ and γ; see Ref. [69] for a comprehensive investigation. In this paper, we are interested in the case in which its energy density passes below zero at high redshifts, which, so far, has not been paid much attention, yet it is the case fitting the scenarios we discussed in the Introduction that most likely address the tensions relevant to H_0 and, in particular, to the high-precision Ly-α data from $z \approx 2.34$. For instance, in the case $\lambda = 0$ ($\rho_{\text{inert}} = \gamma\rho_0$), Eq. (4) reduces to $\rho = \rho_0 - 3\rho_0\gamma\ln a$, consisting of a constant $\rho_0 > 0$ mimicking $\Lambda > 0$ and a

dynamically screening term, $-3\rho_0\gamma \ln a$, in the past for $\gamma < 0$, viz., $\rho_0 - 3\rho_0\gamma \ln a = 0$ at $a = e^{\frac{1}{3\gamma}}$. Yet, the presence of the exponent $\frac{1}{1-\lambda}$ in (4) will allow us to realize such a scenario with additional features.

First, we define $\rho/\rho_0 = x^y$ along with $\rho_0 > 0$, where $x \equiv 1 + 3\gamma(\lambda - 1)\ln a$ and $y \equiv \frac{1}{1-\lambda}$. We note that, unless $\gamma = 0$ (conventional vacuum) or $\lambda = 1$ (perfect fluid with constant EoS parameter), x changes sign at

$$a = a_* \equiv \mathrm{e}^{-\frac{1}{3}\frac{1}{\gamma(\lambda-1)}}, \tag{7}$$

which is in the past ($a_* < 1$, the case we are interested in) for $\gamma(\lambda - 1) > 0$ and in the future ($a_* > 1$) for $\gamma(\lambda - 1) < 0$. Next, $y < 0$ for $\lambda > 1$ so that $\rho \to \pm\infty$ as $a \to a_*$ and $y > 0$ for $\lambda < 1$ so that $\rho \to 0$ as $a \to a_*$, where the latter case is of interest to us. Thus, we proceed with the following two conditions serving our purpose,

$$\lambda < 1 \quad \text{and} \quad \gamma < 0, \tag{8}$$

the latter of which implies $w(a = 1) < -1$; i.e., the gDE must be in the phantom region today.

To get around a mathematical obstacle, when we investigate gDE computationally (see Ref. [102]), we continue by writing $\frac{\rho}{\rho_0} = x^y$ in an equivalent way as $\frac{\rho}{\rho_0} = \mathrm{sgn}(x)|x|^y$ for $y = \frac{m}{n}$ with m and n being odd integers, namely,

$$\rho = \rho_0 \mathrm{sgn}[1 - \Psi \ln a]|1 - \Psi \ln a|^{\frac{1}{1-\lambda}}, \tag{9}$$

for $\Psi \equiv -3\gamma(\lambda - 1) < 0$ (i.e., $\gamma < 0$), $\lambda < 1$ and the exponent $\frac{1}{1-\lambda} = \frac{m}{n}$ with both m and n being odd integers. For practical reasons, we will consider $m = 1$, and so $\lambda = -2N$ with $N = 0, 1, 2, \ldots$, i.e., $\lambda = 0, -2, -4, \ldots$. Here, sgn is the signum function that reads $\mathrm{sgn}(x) = -1, 0, 1$ for $x < 0$, $x = 0$ and $x > 0$, respectively. Of course, in principle, there is an infinite number of such λ values, not continuous, between the ones we listed above, and so we can treat λ in (9) as if it is continuous since one can always find an allowed λ value indistinguishably close to a forbidden λ value.

Consequently, the gDE-CDM model replaces the Λ of the Friedmann equation of the standard ΛCDM model by the gDE (9) serving our purposes and reads

$$\frac{H^2}{H_0^2} = \Omega_{\mathrm{r},0}a^{-4} + \Omega_{\mathrm{m},0}a^{-3} + \Omega_{\mathrm{DE},0}\mathrm{sgn}[1 - \Psi \ln a]|1 - \Psi \ln a|^{\frac{1}{1-\lambda}}, \tag{10}$$

from which we also read off

$$\frac{\rho_{\mathrm{DE}}}{\rho_{\mathrm{c},0}} = \Omega_{\mathrm{DE},0}\mathrm{sgn}[1 - \Psi \ln a]|1 - \Psi \ln a|^{\frac{1}{1-\lambda}}, \tag{11}$$

where $\Psi < 0$ and $\lambda = 0, -2, -4, \ldots$ [for further possibilities, see (9) and the explanations following it]. Here, the subscripts r and m stand for relativistic source ($w_{\mathrm{r}} = \frac{1}{3}$) and dust matter ($w_{\mathrm{m}} = 0$), respectively.

Regarding inertial mass density (5), when $\gamma < 0$, if $1 - \lambda$ is odd, then λ is even, and consequently, we have the exponent $\frac{\lambda}{1-\lambda} = \frac{[\mathrm{even}]}{[\mathrm{odd}]}$ in (5), which in turn implies that $\rho_{\mathrm{inert}} \leq 0$, that is, we can write

$$\rho_{\mathrm{inert}} = \gamma\rho_0|1 + 3\gamma(\lambda - 1)\ln a|^{\frac{\lambda}{1-\lambda}}, \tag{12}$$

under the conditions derived above. It turns out that $\rho_{\mathrm{inert}} = 0$ is the upper bound, viz., $\rho_{\mathrm{inert,max}} = 0$.

We claimed above that gDE can also be viewed as a phenomenological model described by a smooth function that approximately describes the cosmological constant switching sign at a certain redshift and becoming positive just recently in the late Universe. Indeed, under the conditions we consider, $\rho(a = 1) > 0$ and $\rho(a \ll a_*)/\rho(a \gg a_*) \approx -1$ along with $w(a \ll a_*) \approx w(a \gg a_*) \approx -1$, which imply that the energy density of the gDE at high redshifts not only passes below zero but also settles in a value almost equal to the negative of its present time value and remains almost there, say, all the way to the early time before which gDE is irrelevant to the dynamics of the Universe. Note that the EoS parameter is just slightly below (above) the phantom divide line for $a \gg a_*$ ($a \ll a_*$) with $a_* < 1$, and $w \to -1$ only when either $a \to 0$ or $a \to \infty$. Therefore, the energy density of gDE grows very slowly in the future and reaches arbitrarily large values in the very remote future, and also grows in negative values very slowly—obviously, much slower than radiation and dust, both which then eventually dominate gDE in the finite past —with the increasing redshift for $a \ll a_*$, and reaches arbitrarily large negative values in the beginning of the Universe. We note, however, that for arbitrarily large negative values of λ, the energy density equation (11) [or (9)] transforms into a step function,

$$\frac{\rho_{\mathrm{DE}}}{\rho_{\mathrm{c},0}} \to \Omega_{\mathrm{DE},0}\mathrm{sgn}[1 - \Psi \ln a] \quad \text{as } \lambda \to -\infty, \tag{13}$$

with an EoS parameter $w \to -1$. In this case, the energy density of gDE is nondynamical except that it spontaneously changes sign at $a = a_*$. Thus, for large negative values of λ, the gDE model is a very good approximation for describing a cosmological constant spontaneously switching sign at $z = z_*$, namely, in the limit $\lambda \to -\infty$, $\frac{\rho_{\mathrm{DE}}}{\rho_{\mathrm{c},0}} = \Omega_{\mathrm{DE},0}$ for $z < z_*$ and $\frac{\rho_{\mathrm{DE}}}{\rho_{\mathrm{c},0}} = -\Omega_{\mathrm{DE},0}$ for $z > z_*$.

The following may be useful as a demonstration of how the gDE-CDM model works and gives a guide to the values of the parameters of the model. Let us choose $a_* = e^{-1}$ ($z_* \sim 1.7$) in line with Ref. [36] (see Fig. 11 in Ref. [36]). This leads to $\lambda = 1 + \frac{1}{3\gamma}$, where λ must be a large negative number as we must use $\gamma \sim 0$ (it is observationally well known that $\gamma = w_0 + 1 \sim 0$) along with $\gamma < 0$ (our condition

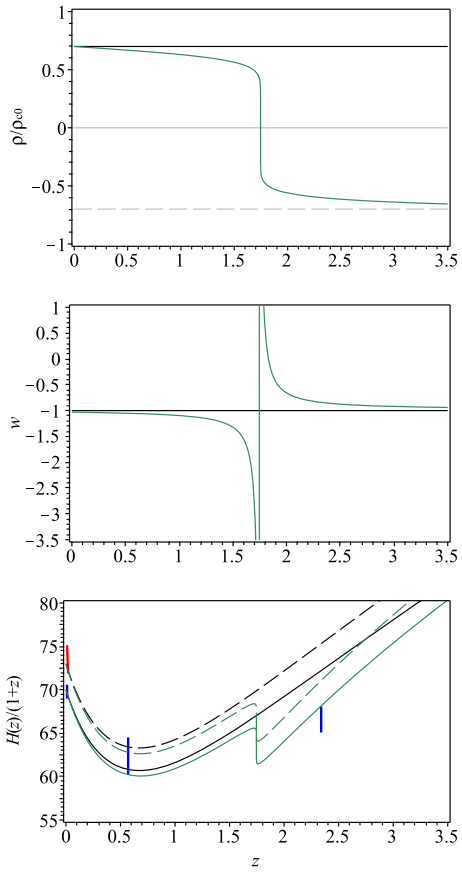

FIG. 1. We use $\Omega_{m,0} = 0.30$ and, for gDE-CDM, $\gamma = -0.03$ along with $\lambda = -10$ (green). $H(z)/(1+z)$ vs z for the gDE-CDM (green) and ΛCDM (black). $H_0 = 70\ \mathrm{km\,s^{-1}\,Mpc^{-1}}$ (solid) and $H_0 = 73\ \mathrm{km\,s^{-1}\,Mpc^{-1}}$ (dashed). $H_0 = 69.8 \pm 0.8\ \mathrm{km\,s^{-1}\,Mpc^{-1}}$ from the TRGB H_0 [22], $H(z = 0.57) = 97.9 \pm 3.4\ \mathrm{km\,s^{-1}\,Mpc^{-1}}$ [103], and $H(z = 2.34) = 222.4 \pm 5.0\ \mathrm{km\,s^{-1}\,Mpc^{-1}}$ from the latest BAO data [35]. $H_0 = 73.52 \pm 1.62\ \mathrm{km\,s^{-1}\,Mpc^{-1}}$ is independent measurement from Gaia parallaxes [20].

derived above). For example, $\gamma = -0.03$ (or $w_0 = -1.03$) predicted by the recent Planck release [9] leads to $\lambda \sim -10$. Accordingly, in Fig. 1, we depict $\frac{\rho(z)}{\rho_{c,0}}$, $w(z)$, and $H(z)/(1+z)$ by considering $\Omega_{m,0} = 0.30$ along with two different Hubble constant values, $H_0 = 70\ \mathrm{km\,s^{-1}\,Mpc^{-1}}$ and $H_0 = 73\ \mathrm{km\,s^{-1}\,Mpc^{-1}}$, for both the ΛCDM model and gDE-CDM model with $\lambda = -10$ and $\gamma = -0.03$. See the previous paragraph for the behaviors of ρ and w beyond our most interested redshift range $z = \{0, 3.5\}$ considered in Fig. 1. We note that, in the gDE-CDM model, the steep change in $H(z)/(1+z)$ at $z \sim z_* = 1.7$—due to the sign change/pole of the energy density/EoS of the gDE—allows it to pass through all data points as well as achieve larger H_0 values, whereas in the case of the ΛCDM model, it does not pass through Ly-α data at $z = 2.34$, and the increased H_0 value worsens this situation. This is signaling that, with respect to the Λ, the gDE would lead to an improved fit to the observational data and alleviate the tensions of various degrees of significance between some existing datasets within the ΛCDM cosmology. As, in the gDE-CDM model, we have $\rho \sim \rho_0$ and $w \lesssim -1$ (slightly in the phantom region) for $z \ll z_*$ (also for $z \sim 0$) and $\rho \sim -\rho_0$ and $w \gtrsim -1$ (slightly in the quintessence region with negative energy density) for $z \gg z_*$, from the phenomenological point of view, such an achievement may be signaling that indeed the cosmological constant is responsible for the current acceleration of the Universe, but it has changed sign at $z_* \sim 2$ and was negative at the higher redshifts.

III. CONSTRAINTS FROM THE LATEST COSMOLOGICAL DATA

This section provides constraints on the gDE-CDM model using the latest observational data with a further discussion of the model and its consequences.

In order to perform the parameter-space exploration, we implement a modified version of the simple and fast Markov chain Monte Carlo code which computes expansion rates and distances from the Friedmann equation named SimpleMC [104] and initially introduced in Ref. [36]. For a comprehensive review of the cosmological parameter inference, see Ref. [105]. The SimpleMC code takes into account a compressed version of recent datasets, for instance the Planck information (PLK) (where the CMB is treated as a "BAO experiment" at redshift $z = 1090$) measured by the angular scale of the sound horizon at that time, a recent analysis of Type Ia supernova (SN) data called Joint Light-Curve Analysis compressed into a piecewise linear function fit over 30 bins evenly spaced in $\log z$, and high-precision baryon acoustic oscillation measurements (BAO), from comoving angular diameter distances, the Hubble distance, and the volume averaged distance, at different redshifts up to $z = 2.36$. For a more detailed description about the datasets used, see Ref. [36]. We also include a collection of currently available cosmic chronometer measurements (H); see Ref. [106].

In this analysis, the radiation content is assumed by considering three neutrino species ($N_{\mathrm{eff}} = 3.046$) with minimum allowed mass $\sum m_\nu = 0.06$ eV and a radiation density parameter given by $\Omega_{r,0} = 2.469 \times 10^{-5} h_0^{-2}(1 + 0.2271 N_{\mathrm{eff}})$, where h_0 is the present-day value of the dimensionless reduced Hubble parameter $h(z) = H(z)/100\ \mathrm{km\,s^{-1}\,Mpc^{-1}}$ [107]. The total radiation content today is kept fixed in our analysis since it is well constrained by the CMB monopole temperature, $T_{\mathrm{CMB},0} = 2.7255 \pm 0.0006$ K [108]. Throughout our analysis, we assume flat priors over our sampling parameters: $\Omega_{m,0} = [0.05, 1.0]$ for the matter (dust) density parameter today, $\Omega_{b,0} h_0^2 = [0.02, 0.025]$ for the physical baryon density parameter, and $h_0 = [0.4, 1.0]$ for the reduced Hubble

TABLE I. Mean values along with 1σ constraints on the set of parameters used to described the gDE-CDM parameters. For one-tailed distributions, the upper limit 95% C.L. is given. For two-tailed distributions, the 68% C.L. is shown. The last column, $-2\ln(\mathcal{L}_{\Lambda,\max}/\mathcal{L}_{\mathrm{gDE},\max})$, is used to compute best-fit differences of gDE-CDM from ΛCDM ($-2\ln\mathcal{L}_{\Lambda,\max} = 73.44$) based on the improvement in the fit alone.

λ	$\Omega_{\mathrm{m},0}$	h_0	$\gamma = w_0 + 1$	Ψ	z_*	t_0 (Gyr)	$-2\Delta\ln\mathcal{L}_{\max}$
ΛCDM	0.302(6)	0.682(5)	0	0	⋯	13.806(22)	0.0
0	0.297(7)	0.689(7)	>-0.08	>-0.25	⋯	13.796(24)	0.02
−2	0.297(7)	0.688(7)	>-0.06	>-0.61	⋯	13.795(25)	0.02
−4	0.289(6), 0.298(7)	0.700(9), 0.686(7)	$-0.057(2)$, >-0.048	$-0.86(3)$, >-0.73	2.31(12),⋯	13.714(25), 13.791(26)	1.0, 0.02
−6	0.292(6), 0.299(6)	0.699(9), 0.685(7)	$-0.039(1)$, >-0.037	$-0.86(3)$, >-0.77	2.31(12),⋯	13.715(25), 13.792(27)	2.0, 0.01
−10	0.294(6), 0.299(6)	0.696(8), 0.684(7)	$-0.025(1)$, >-0.021	$-0.86(3)$, >-0.69	2.32(12),⋯	13.722(27), 13.797(25)	4.4, 0.02
−14	0.296(6), 0.300(6)	0.695(8), 0.683(7)	$-0.019(1)$, >-0.017	$-0.86(3)$, >-0.76	2.33(12),⋯	13.719(31), 13.794(27)	5.3, 0.01
−20	0.297(6), 0.300(6)	0.696(9), 0.683(7)	$-0.013(1)$, >-0.012	$-0.86(3)$, >-0.76	2.32(12),⋯	13.718(31), 13.795(26)	6.0, 0.02
−17.9(5.8)	0.296(6), 0.299(7)	0.697(9), 0.684(8)	$-0.017(8)$, >-0.074	$-0.85(4)$, >-0.69	2.32(19),⋯	13.719(30), 13.795(24)	6.4, 0.01

constant. With regard to the gDE parameters, we assume $\gamma = [-0.2, 0]$ and $\lambda = [-27, 0]$ (when λ is free).

Table I summarizes the observational constraints on the free parameters—$\Omega_{\mathrm{m},0}$, h_0, λ, and γ—as well as the derived parameters—Ψ, z_*, and t_0 (age of the Universe today)—of the gDE-CDM model using the combined datasets PLK + BAO + SN + H, and for comparison shows those parameters used on the standard ΛCDM model ($\gamma = 0$). The columns for each parameter contain the corresponding mean values and 1σ errors, according to the number of modes presented on the one-dimensional (1D) marginalized posterior distributions. In the last column, we list the $-2\Delta\ln\mathcal{L}_{\max} = \Delta\chi^2_{\min}$ values representing the improvement in the fit to the data with respect to the ΛCDM. At the outset, we immediately notice that in our analyses the gDE leads to an improvement of up to $\Delta\chi^2_{\min} = 6.4$ (corresponding to about 2.5σ) with respect to the cosmological constant. In what follows, we discuss in detail how this significant improvement is due to the fact that the gDE-CDM alleviates some of the tensions the ΛCDM experiences.

In Table I, for $\lambda = 0, -2$, we observe nothing interesting and no significant improvement to the fit with respect to ΛCDM, viz., $\Delta\chi^2_{\min} < 0.02$. However, we observe something surprising occurs when $\lambda \leq -4$ (also when λ is free), that the data predict bimodal posterior probability distributions for the parameters of the gDE-CDM, for which we observe two sets of constraint values in each column of Table I. This may also be seen, for example, from the top left panel of Fig. 2, which displays 1D marginalized posterior distributions for the γ parameters. Notice that, for $\lambda \leq -4$, as we move toward the larger negative values of γ, the existence of a second (new) maximum starts appearing significantly far away from $\gamma = 0$ (ΛCDM). The first (old) maximum containing $\gamma = 0$ is always there, but, when $\lambda \leq -6$, it consistently shrinks with the larger negative values of λ, during which the new maximum is getting relatively higher and sharper. This implies that the data significantly favor the new maximum over the old maximum when $\lambda \lesssim -6$. Indeed, we read from Table I that the improvement in the fit with respect to ΛCDM reaches highly significant levels—e.g., $\Delta\chi^2_{\min} = 6$ when $\lambda = -20$ and $\Delta\chi^2_{\min} = 6.4$ when λ is free—for the new maximum, while it remains always at insignificant levels —$\Delta\chi^2_{\min} \lesssim 0.02$ irrespective of the value of λ—for the old maximum. The poor improvement level of $\Delta\chi^2_{\min} \lesssim 0.02$ both in the old maximum (the maximum containing $\gamma = 0$ when $\lambda \lesssim -4$ and λ is free and the single maximum when $\lambda \lesssim 3$) presents no evidence for favoring these over the ΛCDM, and the constraints on the parameters for these cases do not show a considerable deviation from those of

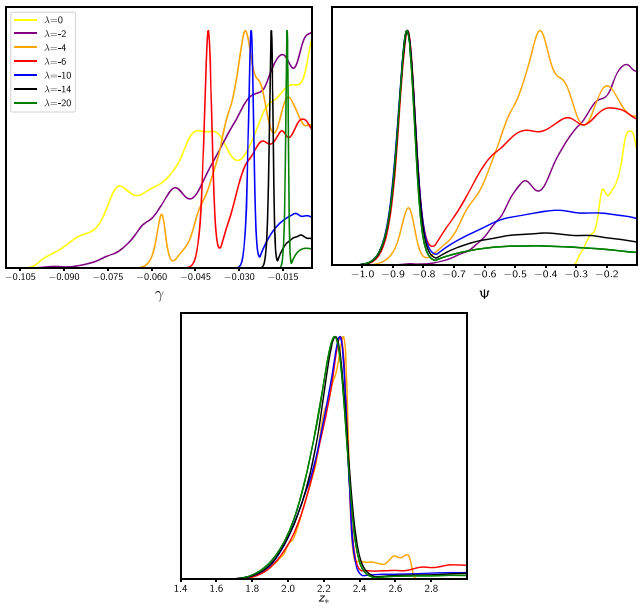

FIG. 2. 1D marginalized posterior distributions for the graduated γ parameter (top left panel), $\Psi \equiv 3\gamma(1-\lambda)$ (right), and the redshift location of the pole (if present) given by Eq. (14). For a better display, we have included some particular cases of λ values.

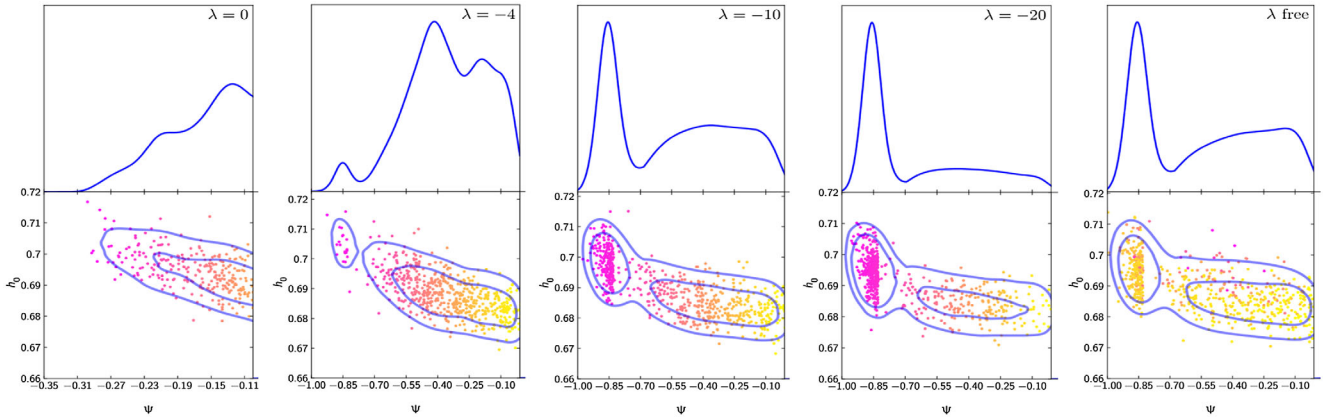

FIG. 3. Top panel: 1D marginalized posterior distributions of Ψ, along with (bottom panel) 2D posterior distributions of $\{\Psi, h_0\}$ color coded by the γ parameter.

the ΛCDM. Therefore, in what follows, we discard all these cases and proceed in our discussions with reference to the ΛCDM ($\gamma = 0$), basically, by considering only the new maximum that appears when $\lambda \lesssim -6$, e.g., by considering the one on the left of the pair of constraints given in a column for a parameter of the gDE-CDM in Table I.

The presence of these new maxima has important consequences and may be better explained through the expression (7). This expression indicates if there exists a sign change in the energy density of the gDE (or a pole in its EoS parameter), it will happen at a redshift

$$z_* = e^{-\frac{1}{\Psi}} - 1. \tag{14}$$

Hence, the quantity $\Psi = -3\gamma(\lambda - 1)$ determines the position of the pole and, if it is a real one, must yield a unique value irrespective of the values λ and γ. That is, for a given λ, the γ parameter selects its best position such that Ψ remains unchanged, and this can be seen in the right-hand panel of Fig. 2 (see also Table I). We observe that a peak at $\Psi = -0.86$—significantly away from $\Psi = 0$ (ΛCDM)—emerges when $\lambda = -4$ and as λ takes more negative values (see the cases $\lambda \leq -6$) it becomes significantly higher and sharper, fixed at $\Psi = -0.86$, while the old peak containing $\Psi = 0$ becomes more prolate and lower. This implies highly significant observational evidence for the sign change of the energy density of the gDE (or pole in its EoS parameter) at the redshift corresponding to $\Psi = -0.86$. We have shown, according to (14), in the bottom panel of Fig. 2, the 1D marginalized posterior distribution of the redshift for this event persistently located at $z_* \approx 2.32$ (see Table I). Interestingly, but not surprisingly, this particular position agrees with the location of the Ly-α auto- and cross-correlation BAO ($z = 2.34$) data and the works [35–37]. This suggests such a behavior of DE for alleviating the tensions besetting this observation. We should note here that the peaks containing $\Psi = 0$ (ΛCDM) also predict the sign change of the gDE, but we have discarded them for the following reasons. First, these cases correspond to the ones we have discarded above, since they do not present any statistical evidence for being favored over ΛCDM (the $\Psi \to 0$ limit leading to $z_* \to \infty$). Second, in our analyses, we observe that these cases predict completely different z_* values for different λ values (if they were real, the predictions need to have been stable at a certain redshift), all of which are extremely large (even having redshift values larger than the redshift of the big bang nucleosynthesis epoch) at which dark energy is irrelevant to the cosmological dynamics.

The bimodal distribution that Ψ exhibits has a strong impact on the posterior distribution of h_0, and therefore on the Hubble constant H_0, which also exhibits a bimodal behavior. Figure 3 describes this behavior; as soon as the λ parameter starts decreasing, the bimodal distribution on the panel $\{h_0, \Psi\}$ starts showing up for a particular γ value (display in pink color). This bimodal distribution is summarized on the marginalized error bars shown in Fig. 4. We observe that, while the values (green) associated

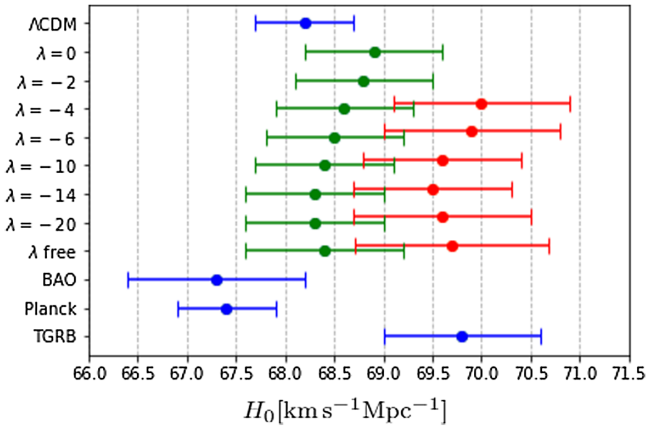

FIG. 4. Means values along with 1σ error bars from the 1D marginalized posterior distributions of $H_0[\mathrm{km\,s^{-1}\,Mpc^{-1}}]$. Green error bars are associated with the peak containing $\Psi \sim 0$ (ΛCDM), whereas red one are associated with the new peak stable at $\Psi \sim -0.86$.

with the old peak containing $\Psi \sim 0$ (ΛCDM) agree with the H_0 values measured from the inverse distance ladder (e.g., $H_0 = 67.4 \pm .5$ from Planck 2018 [9]), the ones (red) associated with the new peak stable at $\Psi \sim -0.86$ (away from $\Psi = 0$) agree with the higher H_0 values measured from the distance ladder measurements (e.g., $H_0 = 69.8 \pm 0.8$ from a recent calibration of the tip of the red giant branch (TRGB) applied to Type Ia supernovae [22]). Therefore, the H_0 predicted within the ΛCDM (matching our results from the old peak) has deficiency with respect to the TRGB H_0 value, while the ones predicted by the new peak (appears for $\lambda \lesssim -4$) perfectly match with it. It certainly favors the new peak that predicts a value matching the independent TRGB H_0 value. It is also significant that it uses the distance ladder approach, rather than the inverse distance ladder approach. Also, the latter BAO calibration of H_0 is not completely independent of the Planck measurement, as both H_0 determinations are based on the ΛCDM and its adopted value of the sound horizon scale. Moreover, the independent TRGB H_0 value (so, the values from our new peak) agrees with both Planck [9] and Cepheid [19–21] H_0 values. However, when combined with Cepheid measurements, the tension with the Planck value is relieved only at about 1σ level and still remains significant [22].

We notice in Table I that the values of the parameters $\Psi(\gamma, \lambda)$—or $z_*(\gamma, \lambda)$—and of the other cosmological parameters Ω_0, h_0, and t_0 are quite stable for $\lambda \leq -10$. One may see from the last row in Table I that we confirm this observation when we constrain the model by letting also the parameter λ be free (we use flat prior $\lambda = [-27, 0]$). The left panel of Fig. 5 displays the three-dimensional (3D) marginalized posterior distribution of the $\{\Psi, \lambda\}$ parameter region color coded with the γ parameter. Here, the bimodality of the constraints on the gDE-CDM shows up as two detached two-dimensional (2D) outer contours. The narrow one located at $\Psi \sim -0.86$ corresponds to the new maximum, while the wide one corresponds to the old maximum containing the ΛCDM (top-right corner). In the right panel of the same figure, we present the 1D posterior distribution of the z_* associated with the new maximum, which demonstrates that the redshift at which the gDE energy density changes sign (its EoS parameter exhibits a pole) is stable at $z_* \sim 2.32$.

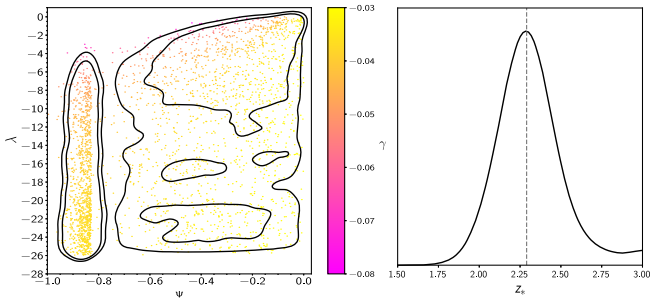

FIG. 5. Graduated dark energy model with varying the λ parameter. Left panel: 3D marginalized posterior distributions for the graduated λ and Ψ parameters, color coded by the γ parameter. Right panel: 1D marginalized posterior of the redshift position given by the pole. The vertical line is the mean value $z_* = 2.32$.

It was shown in Ref. [37] through the Omh^2 diagnostic (introduced to test the Λ hypothesis in a model-independent way) that the ΛCDM is in tension with the BAO's statistically independent measurements of $H(z)$ at redshifts of 0.57 and 2.34. It was shown that this tension is alleviated in models in which the Λ was dynamically screened (compensated) in the past and that the energy density of such evolving DE models passes below zero (exhibits a pole in the effective EoS) at $z \sim 2.4$. These are in line with the new maxima of the gDE-CDM, yet in addition, the fact that the constant that plays the role of Λ in gDE is embedded into a set of parentheses raised to a power renders our model more featured. Therefore, we also investigate gDE in the context of the Omh^2 diagnostic.

The Omh^2 diagnostic is defined in Ref. [37] as follows,

$$Omh^2(z_i; z_j) = \frac{h^2(z_i) - h^2(z_j)}{(1+z_i)^3 - (1+z_j)^3}, \tag{15}$$

and depends only on $H(z)$. Accordingly, knowing it at two or more redshifts, one can obtain Omh^2 value(s) in a model-independent manner and thence conclude whether or not the DE is a Λ. For the ΛCDM, omitting radiation (negligible in the late Universe), we have $h^2 = h_0^2[\Omega_{\mathrm{m},0}(1+z)^3 + 1 - \Omega_{\mathrm{m},0}]$ leading to a constant

$$Omh^2(z_i; z_j) = h_0^2 \Omega_{\mathrm{m},0}. \tag{16}$$

For the gDE-CDM, using (10), we have

$$Omh^2(z_i; z_j) = h_0^2 \Omega_{\mathrm{m},0} + h_0^2 (1 - \Omega_{\mathrm{m},0}) \frac{\mathrm{sgn}(x_i)|x_i|^y - \mathrm{sgn}(x_j)|x_j|^y}{(1+z_i)^3 - (1+z_j)^3}, \tag{17}$$

where have neglected radiation and used the zero-curvature constraint, $\Omega_{\mathrm{m},0} + \Omega_{\mathrm{DE},0} = 1$. The second line of the $Omh^2(z_i; z_j)$ for the gDE-CDM emerges as a correction to the one for the ΛCDM. We can calculate the predicted $Omh^2(z_i; z_j)$ with these two equations for any pair of chosen redshifts using the constraints on the models and then compare the same with the model-independent estimates obtained by (15).

We calculate, from (15), the model-independent estimates as $Omh^2(z_1; z_2) = 0.164 \pm 0.024$, $Omh^2(z_1; z_3) = 0.123 \pm 0.006$, and $Omh^2(z_2; z_3) = 0.119 \pm 0.007$ by using $H(z_1 = 0) = 69.8 \pm 0.8\ \mathrm{km\,s^{-1}\,Mpc^{-1}}$ from the

TABLE II. Mean values along with $1-\sigma$ constraints on the set of parameters that describe Omh^2 diagnostic.

λ	$Omh^2(z_1;z_2)$	$Omh^2(z_1;z_3)$	$Omh^2(z_2;z_3)$
ΛCDM	0.140(2)	0.140(2)	0.140(2)
0	0.134(4)	0.139(4)	0.140(4)
−2	0.135(4)	0.140(2)	0.140(2)
−4	0.136(3)	0.129(1), 0.140(2)	0.129(2), 0.140(2)
−6	0.137(2)	0.128(1), 0.140(3)	0.127(2), 0.140(2)
−10	0.137(2), 0.139(2)	0.127(2), 0.140(2)	0.123(2), 0.140(2)
−14	0.138(2), 0.139(2)	0.126(2), 0.140(2)	0.127(2), 0.140(2)
−20	0.139(2), 0.140(2)	0.125(2), 0.140(2)	0.124(2), 0.140(2)
Free	0.136(4), 0.139(2)	0.127(4), 0.140(2)	0.126(2), 0.140(2)

TRGB H_0 [22], $H(z_2=0.57)=97.9\pm3.4\ \mathrm{km\,s^{-1}\,Mpc^{-1}}$ based on the clustering of galaxies in the Sloan Digital Sky Survey (SDSS)-III, Baryon Oscillation Spectroscopic Survey (BOSS), Data Release 11 (DR11) [103], and $H(z_3=2.34)=222.4\pm5.0\ \mathrm{km\,s^{-1}\,Mpc^{-1}}$ based on the BAO in the Ly-α forest of SDSS DR11 data [35]. We notice that the constraint $Omh^2=0.140\pm0.002$ ($Omh^2=0.143\pm0.001$ in Planck 2018 [9]) we obtained for the ΛCDM is in clear tension with the latter two of these estimates. We see in Table II that, for $\lambda\leq-10$ as well as the λ free case, the constraints for all of the three Omh^2 exhibit bimodal characteristics; i.e., there are two valued constraints corresponding to the new (left) and old (right) maxima. We notice $Omh^2(z_1;z_2)\sim0.140$ (as in the ΛCDM) is almost the same for both the new and old maxima, yet it agrees with the corresponding model-independent estimate. However, when we consider $Omh^2(z_1;z_3)$ and $Omh^2(z_2;z_3)$, we observe that, while the ones associated with the new maximum yield approximately 0.125 in agreement with the corresponding model-independent estimates, the ones associated with the old maximum yield $\approx$ 0.140 in tension. For a visual demonstration, in Fig. 6, we show the marginalized posterior distributions for the parameter γ in the $\{\gamma, Omh^2(z_i;z_j), h_0\}$ subspace for $\{z_1,z_2\}$, $\{z_1,z_3\}$ and $\{z_2,z_3\}$, where the blue contours and 3D scatter color plots described the gDE-CDM model for $\lambda=-20$. The color code indicates the value of γ labeled by the color bar. Black contours display 2D marginalized posterior distributions for the ΛCDM which agree with the position of the yellow points corresponding to the old maxima of the gDE-CDM. The contours at about $Omh^2\sim0.125$ correspond to the new maxima of the gDE-CDM describing the case in which the energy density of the gDE passes below zero at $z\sim2.32$.

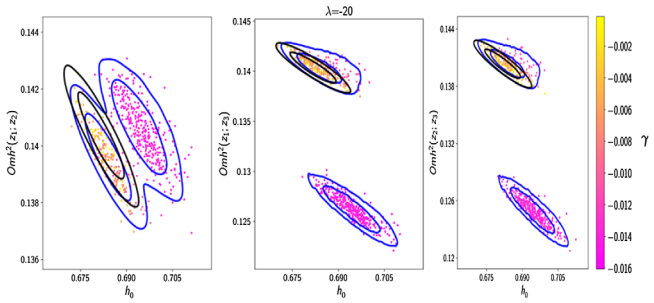

FIG. 6. Omh^2 diagnostic for the graduated dark energy model with $\lambda=-20$ using three redshifts $\{z_1,z_2\}$ (left), $\{z_1,z_3\}$ (middle), and $\{z_2,z_3\}$ (right). The color code indicates the value of γ parameter, where the yellow points mimic the ΛCDM behavior and the pink ones the new feature introduced by the gDE model.

All these superiorities in the goodness of fit to the observational data arising in the case of the new maxima of the gDE-CDM are obviously consequences of the fact that the energy density of the gDE passes below zero at $z_*\approx2.3$ by exhibiting a certain type of dynamics. By using the FGIVENX package [109], we show in the upper panel of Fig. 7 the probability (the more pink implies more probable) distribution of the redshift dependency of the energy density of gDE scaled to the critical energy density of the present-day Universe, viz., $\rho_{\rm DE}/\rho_{\rm c,0}$. We observe that gDE, viz., $\rho_{\rm DE}(z)/\rho_{\rm c,0}$, does not distinguish from Λ (solid straight black line) at a value approximately 0.70 for $z\lesssim2$, but it reaches a junction at $z\sim2.3$, and for larger redshifts, it either keeps tracking Λ by retaining the value approximately 0.70 (the one associated with the old maximum and disfavored by the data) or rapidly changes route and starts to track a new value approximately −0.70 like a mirror image of the former track at $\rho_{\rm DE}=0$ (the case associated with the new maximum and favored by the data). The rapid sign switch of the gDE energy density at $z\sim2.3$ implies a rapid drop in the total energy density of the Universe, and in $H(z)$, at that redshift. This behavior of $H(z)$ emerges in association with the new maxima of the gDE-CDM for more negative values of λ, as can be seen in the lower panel of Fig. 7. This reconciles it with the lower $H(z)$ value of the Ly-α data at $z=2.34$ with respect to the one predicted by ΛCDM for that redshift. Furthermore, this reconciliation between the gDE-CDM and Ly-α data, in turn, provides the gDE-CDM with easiness in achieving large $H(z)$ values for $z\lesssim2$ and thereby predicts larger H_0, and so gDE-CDM relieves the H_0 tension that ΛCDM has been suffering from.

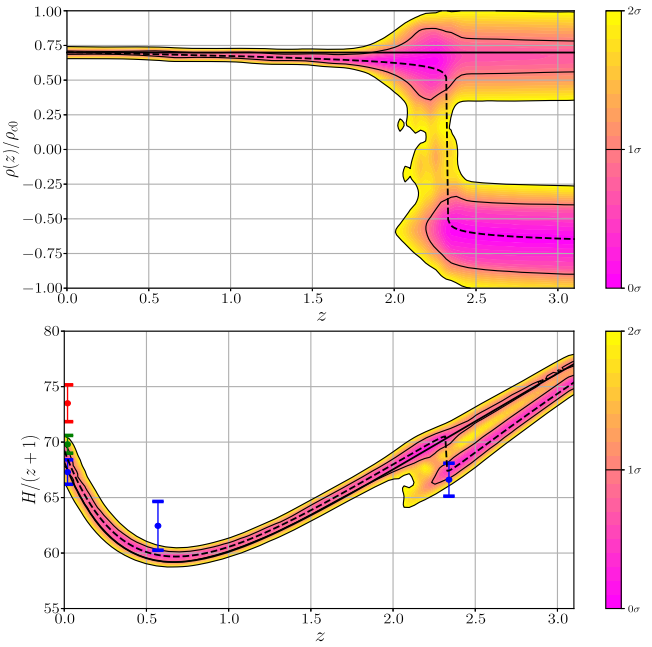

FIG. 7. Top panel: $\rho_{\rm gDE}/\rho_{\rm c0}$ vs redshift z for $\lambda = -20$ displays the maximum predicted that $\rho_{\rm gDE}$ changes sign at $z \sim 2.3$. Bottom: $H(z)/(1+z)$ function. Included are the latest BAO data points [36] (blue bars) where $H_0 = 67.3 \pm 1.1$, the Planck 2018 [9] $H_0 = 67.4 \pm 0.5$ data (red bar), and the TGRB model-independent [22] $H_0 = 69.8 \pm 0.8$ data (green bar). The black dashed line corresponds to best-fit values of gDE, and the solid black line corresponds to ΛCDM. We note that, due to the jump at $z \sim 2.3$, the gDE model is not in tension with the BAO Ly-α data from $z = 2.34$ in contrast to ΛCDM model and also gDE gives larger H_0 values with respect to ΛCDM model and thereby relaxes H_0 tension.

IV. SPONTANEOUS SIGN SWITCH IN THE COSMOLOGICAL CONSTANT

In this section, we would like to continue by commenting on the implication of the dynamics of gDE that leads to all these reconciliations with the observational data on the nature of the dark energy. First, we note the following features of gDE that we have further understood upon confronting the observational data. We read off from Table I that, for larger negative values of λ, $\rho_{\rm DE}/\rho_{\rm c,0} = 0.70$, and $w_0 \sim -1.01$ (i.e., in the phantom region but very close to the conventional vacuum energy) at $z = 0$, its energy density switches sign rapidly (almost spontaneously) at $z_* \approx 2.32$ (which is quite stable) and settles into a value $\rho_{\rm DE}/\rho_{\rm c,0} \sim -0.70$ (the opposite of its present-day value) and remains ($w_{\rm DE} \approx -1$) there for $z_* \gtrsim 2.3$. Next, we observe in the same table that the larger the negative values of λ, the better the fit to the data (the larger $\Delta\chi^2_{\rm min}$). This follows the trend that makes $\rho_{\rm DE}(z)$ increasingly resemble a step function centred at z_* with two branches yielding opposite values about zero—a pattern of flat positive energy density for $z < z_*$ and flat negative energy density for $z > z_*$, both of which have the same absolute value—and indeed, we know from (13), that $\rho_{\rm DE}$ transforms into a step function for arbitrarily large negative values of λ. The largest negative λ value we considered in our analyses is -27, yet it is easy to check mathematically that considering even larger negative values would not affect our results considerably since, for this value, the function $\rho_{\rm DE}(z)$ already closely resembles a step function. Thus, our results from the new maximum of the gDE for large negative values of λ can safely be interpreted as the results one would obtain for a cosmological constant that achieved its present-day positive value by spontaneously switching sign at $z_* \sim 2.3$, but was negative in the earlier stage of the Universe.

Some general constraints that are typically applied to the classical matter source, irrespective of its detailed description, may be utilized for further supporting our interpretation (see Refs. [61,110]). Let us consider gDE as an actual barotropic fluid, $p = p(\rho)$, along with the best fit values obtained on its free parameters from the observational analysis. In this case, although it behaves almost like a cosmological constant (in spite of the fact that it switches sign at $z \approx 2.32$) throughout the history of the Universe, strictly speaking, it violates the weak energy condition, namely, the non-negativity conditions on the energy density, $\rho \geq 0$, for $z > z_*$, and on the inertial mass density, $\rho_{\rm inert} \geq 0$, throughout the history of the Universe. Moreover, there are periods during which it violates the condition $0 \leq c_s^2 \leq 1$ on the speed of sound of a barotropic fluid given by the adiabatic formula $c_s^2 = {\rm d}p/{\rm d}\rho$. The upper limit (causality limit) is a rigorous one which cannot be violated unless we abandon relativity theory. The lower limit applies to a stable situation, and otherwise the fluid is classically unstable against small perturbations of its background energy density—the so-called Laplacian (or gradient) instability. It is well known that phenomenological fluid models of DE are difficult to motivate, and adiabatic fluid models are typically unstable against perturbations, since c_s^2 is usually negative for $w < 0$. It is possible to evade this constraint in nonadiabatic fluid descriptions (e.g., canonical scalar field for which the effective speed of sound—which governs the growth of inhomogeneities in the fluid—is equal to unity, $c_{s\,\rm eff} = 1$), and in an adiabatic fluid if w decreases sufficiently fast as the Universe expands (e.g., Chaplygin gas). However, with some exceptions, it is unlikely to describe gDE with a canonical scalar field—especially when we consider the best fit values. Also, gDE yields $c_s^2 = -1 + \gamma\lambda(\frac{\rho}{\rho_0})^{\lambda-1} = -1 + \frac{\gamma\lambda}{1+3\gamma(\lambda-1)\ln a}$, and $c_s^2(z=0) = -1 + \gamma\lambda$. Accordingly, the constrains we obtained when λ is free predict $c_s^2(z=0) = -0.6957 \pm 0.1739$ for $z = 0$ and $c_s^2 \gg 1$ while $0 < \rho \ll \rho_0$ (just after gDE assumes positive values at $z \approx 2.32$). On the other hand, whether it is positive or negative, a cosmological constant [viz., the limit $\lambda \to -\infty$; see (13)] is well behaved:

$\rho_{\rm inert} = 0$, and $c_s^2 = 0$ (it has no speed of sound, and thereby does not support classical fluctuations). Regarding the negativity of its energy density (when $z > z_*$), a negative cosmological constant is ubiquitous in the fundamental theoretical physics without any complication; for instance, it can be taken as just a geometrical component ($\rho < 0$ will then be an effective energy density rather than an actual one), and it also is very natural from symmetry considerations and provides the ground state (AdS background) in various low energy limits of string theory.

Thus, bringing all these points together, it is tempting to conclude that the cosmological constant has spontaneously switched sign and become positive at $z \approx 2.32$ and triggered the late-time acceleration. Of course, one could look for realizing such a nontrivial behavior of gDE as an effective source in a modified gravity model (the general constraints that are typically applied to classical matter source might then be evaded) and reach different conclusions.

V. CONCLUSIONS

We have considered a type of dark energy that can be viewed as characterizing the minimum dynamical deviation from the null inertial mass density—described by the conventional vacuum (or cosmological constant, Λ)—in the form $\rho_{\rm inert} \propto \rho^{\lambda}$ with λ being a constant. This source, we called graduated dark energy, presents a wide variety of dynamics which were first studied in the context of inflaton [65–67] and more recently of dark energy [68–71]. We focused on its dynamics (which has not been studied in detail so far) that emerges when $\rho_{\rm inert} < 0$, and $\lambda < 1$ is written as a ratio of two odd integers. In this case, it yields an energy density that dynamically assumes negative values in the recent past, in line, for instance, with Refs. [26–31, 35–37]. They proposed such models to address, for instance, the persistent tensions arising between the cosmological constant hypothesis of the standard ΛCDM model and the model-independent H_0 measurements and/or high-precision Ly-α measurements of BAO. Importantly, for large negative values of λ, gDE presents a phenomenological model described by a smooth function. It approximately describes the cosmological constant spontaneously switching sign at a certain redshift to become positive quite recently in the late Universe. In particular, it transforms into a step function for arbitrarily large negative λ values.

We have confronted the gDE-CDM model, replaced the Λ hypothesis by the gDE, with the latest combined observational data sets of PLK + BAO + SN + H. We have observed that something striking occurs when $\lambda \leq -4$ (also when λ is free); the data predict bimodal posterior probability distributions for the parameters of the gDE-CDM model: new maxima significantly far away from $\gamma = 0$ (ΛCDM) and old maxima containing $\gamma = 0$. The improvement in the goodness of the fit with respect to the Λ reaches highly significant levels—e.g., $\Delta\chi^2_{\rm min} = 6$ when $\lambda = -20$ and $\Delta\chi^2_{\rm min} = 6.4$ when λ is free—for the new maxima, while it remains always at insignificant levels—$\Delta\chi^2_{\rm min} \lesssim 0.02$, irrespective of the value of λ—for the old maxima. We have shown that, in contrast to the old maxima covering the ΛCDM model, these new maxima of the gDE-CDM model also agree with the model-independent H_0 measurements, high-precision Ly-α data, and model-independent Omh^2 diagnostic estimates.

We have demonstrated that the superior features endowed by the new maxima of the gDE-CDM model are due to the energy density of the gDE rapidly changing sign at the redshift $z \approx 2.3$ (shown to be quite stable in our observational analysis), and this in turn leads to a rapid drop in the total energy density of the Universe, and in $H(z)$, at the same redshift. It has turned out that this happens for large negative values of λ, which renders the redshift dependency of the gDE density close to a step function, which to a good approximation describes a cosmological constant spontaneously switching sign. Therefore, our findings, by means of gDE in the light of observational data, provide strong hints of a spontaneous sign switch in the cosmological constant. This leads us to conjecture that the cosmological constant has spontaneously switched sign and become positive, namely, the Universe has transitioned from AdS vacua to dS vacua, at $z \approx 2.32$, and triggered the late-time acceleration. This suggests looking for such mechanisms in string theory constructions. The fact that constructing metastable dS and/or AdS in string theory occupies a key place in the string theory investigations indicates that the future confirmation or falsification of our conjecture would have far reaching implications for fundamental theoretical physics as well as for the identity of the dark energy.

ACKNOWLEDGMENTS

The authors thank to Dragan Huterer, Paolo Creminelli, Jorge Noreña, and Mehmet Ozkan for valuable discussions. Ö. A. acknowledges the support by the Turkish Academy of Sciences in scheme of the Outstanding Young Scientist Award (TÜBA-GEBİP). Ö. A. is grateful for the hospitality of the Abdus Salam International Center for Theoretical Physics (ICTP) while the part of this research was being carried out. J. D. B. was supported by the STFC of the UK. J. A. V. acknowledges the support provided by FOSEC SEP-CONACYT Investigación Básica Grant No. A1-S-21925 and UNAM-DGAPA-PAPIIT Grant No. IA102219.

[1] A. A. Starobinsky, A new type of isotropic cosmological models without singularity, Phys. Lett. B **91**, 99 (1980), Adv. Ser. Astrophys. Cosmol. **3**, 130 (1987).

[2] A. H. Guth, The inflationary Universe: A possible solution to the horizon and flatness problems, Phys. Rev. D **23**, 347 (1981); Adv. Ser. Astrophys. Cosmol. **3**, 139 (1987).

[3] A. D. Linde, A new inflationary Universe scenario: A possible solution of the horizon, flatness, homogeneity, isotropy and primordial monopole problems, Phys. Lett. **108B**, 389 (1982); Adv. Ser. Astrophys. Cosmol. **3**, 149 (1987).

[4] A. Albrecht and P. J. Steinhardt, Cosmology for Grand Unified Theories with Radiatively Induced Symmetry Breaking, Phys. Rev. Lett. **48**, 1220 (1982); Adv. Ser. Astrophys. Cosmol. **3**, 158 (1987).

[5] A. G. Riess *et al.* (Supernova Search Team), Observational evidence from supernovae for an accelerating universe and a cosmological constant, Astron. J. **116**, 1009 (1998).

[6] P. A. R. Ade *et al.* (Planck Collaboration), Planck 2015 results. XIII. Cosmological parameters, Astron. Astrophys. **594**, A13 (2016).

[7] S. Alam *et al.* (BOSS Collaboration), The clustering of galaxies in the completed SDSS-III Baryon Oscillation Spectroscopic Survey: Cosmological analysis of the DR12 galaxy sample, Mon. Not. R. Astron. Soc. **470**, 2617 (2017).

[8] T. M. C. Abbott *et al.* (DES Collaboration), Dark energy survey year 1 results: Cosmological constraints from galaxy clustering and weak lensing, Phys. Rev. D **98**, 043526 (2018).

[9] N. Aghanim *et al.* (Planck Collaboration), Planck 2018 results. VI. Cosmological parameters, arXiv:1807.06209.

[10] S. Weinberg, The cosmological constant problem, Rev. Mod. Phys. **61**, 1 (1989).

[11] V. Sahni and A. A. Starobinsky, The case for a positive cosmological Lambda term, Int. J. Mod. Phys. D **09**, 373 (2000).

[12] P. J. E. Peebles and B. Ratra, The cosmological constant and dark energy, Rev. Mod. Phys. **75**, 559 (2003).

[13] T. Padmanabhan, Cosmological constant: The weight of the vacuum, Phys. Rep. **380**, 235 (2003).

[14] J. S. Bullock and M. Boylan-Kolchin, Small-scale challenges to the ΛCDM paradigm, Annu. Rev. Astron. Astrophys. **55**, 343 (2017).

[15] W. L. Freedman, Cosmology at a crossroads, Nat. Astron. **1**, 0121 (2017).

[16] M. Raveri and W. Hu, Concordance and discordance in cosmology, Phys. Rev. D **99**, 043506 (2019).

[17] E. Di Valentino, Crack in the cosmological paradigm, Nat. Astron. **1**, 569 (2017).

[18] G. B. Zhao *et al.*, Dynamical dark energy in light of the latest observations, Nature (London) **1**, 627 (2017).

[19] A. G. Riess *et al.*, A 2.4% determination of the local value of the Hubble constant, Astrophys. J. **826**, 56 (2016).

[20] A. G. Riess *et al.*, Milky Way Cepheid standards for measuring cosmic distances and application to Gaia DR2: Implications for the Hubble constant, Astrophys. J. **861**, 126 (2018).

[21] A. G. Riess, S. Casertano, W. Yuan, L. M. Macri, and D. Scolnic, Large magellanic cloud Cepheid Standards provide a 1% foundation for the determination of the Hubble constant and stronger evidence for physics beyond ΛCDM, Astrophys. J. **876**, 85 (2019).

[22] W. L. Freedman *et al.*, The Carnegie-Chicago Hubble program. VIII. An independent determination of the Hubble constant based on the tip of the red giant branch, Astrophys. J. **882**, 34 (2019).

[23] S. Vagnozzi, S. Dhawan, M. Gerbino, K. Freese, A. Goobar, and O. Mena, Constraints on the sum of the neutrino masses in dynamical dark energy models with $w(z) \geq -1$ are tighter than those obtained in ΛCDM, Phys. Rev. D **98**, 083501 (2018).

[24] E. Di Valentino, R. Z. Ferreira, L. Visinelli, and U. Danielsson, Late time transitions in the quintessence field and the H_0 tension, Phys. Dark Universe **26**, 100385 (2019).

[25] E. Di Valentino, A. Melchiorri, and J. Silk, Cosmological constraints in extended parameter space from the Planck 2018 Legacy release, J. Cosmol. Astropart. Phys. 01 (2020) 013.

[26] L. Visinelli, S. Vagnozzi, and U. Danielsson, Revisiting a negative cosmological constant from low-redshift data, Symmetry **11**, 1035 (2019).

[27] E. Mörtsell and S. Dhawan, Does the Hubble constant tension call for new physics?, J. Cosmol. Astropart. Phys. 09 (2018) 025.

[28] V. Poulin, K. K. Boddy, S. Bird, and M. Kamionkowski, Implications of an extended dark energy cosmology with massive neutrinos for cosmological tensions, Phys. Rev. D **97**, 123504 (2018).

[29] S. Capozziello, Ruchika, and A. A. Sen, Model independent constraints on dark energy evolution from low-redshift observations, Mon. Not. R. Astron. Soc. **484**, 4484 (2019).

[30] Y. Wang, L. Pogosian, G. B. Zhao, and A. Zucca, Evolution of dark energy reconstructed from the latest observations, Astrophys. J. **869**, L8 (2018).

[31] K. Dutta, Ruchika, A. Roy, A. A. Sen, and M. M. Sheikh-Jabbari, Beyond ΛCDM with low and high Redshift data: Implications for dark energy, Gen. Relativ. Gravit. **52**, 15 (2020).

[32] A. Banihashemi, N. Khosravi, and A. H. Shirazi, Ups and downs in dark energy: Phase transition in dark sector as a proposal to lessen cosmological tensions, arXiv:1808.02472.

[33] A. Banihashemi, N. Khosravi, and A. H. Shirazi, Ginzburg-Landau theory of dark energy: A framework to study both temporal and spatial cosmological tensions simultaneously, Phys. Rev. D **99**, 083509 (2019).

[34] G. Ye and Y. S. Piao, Is the Hubble tension a hint of AdS around recombination? arXiv:2001.02451.

[35] T. Delubac *et al.* (BOSS Collaboration), Baryon acoustic oscillations in the Lyα forest of BOSS DR11 quasars, Astron. Astrophys. **574**, A59 (2015).

[36] É. Aubourg *et al.*, Cosmological implications of baryon acoustic oscillation measurements, Phys. Rev. D **92**, 123516 (2015).

[37] V. Sahni, A. Shafieloo, and A. A. Starobinsky, Model independent evidence for dark energy evolution from Baryon acoustic oscillations, Astrophys. J. **793**, L40 (2014).

[38] E. J. Copeland, M. Sami, and S. Tsujikawa, Dynamics of dark energy, Int. J. Mod. Phys. D **15**, 1753 (2006).
[39] R. R. Caldwell and M. Kamionkowski, The physics of cosmic acceleration, Annu. Rev. Nucl. Part. Sci. **59**, 397 (2009).
[40] T. Clifton, P. G. Ferreira, A. Padilla, and C. Skordis, Modified gravity and cosmology, Phys. Rep. **513**, 1 (2012).
[41] A. De Felice and S. Tsujikawa, $f(R)$ theories, Living Rev. Relativity **13**, 3 (2010).
[42] S. Capozziello and M. De Laurentis, Extended theories of gravity, Phys. Rep. **509**, 167 (2011).
[43] S. Nojiri, S. D. Odintsov, and V. K. Oikonomou, Modified gravity theories on a nutshell: Inflation, bounce and late-time evolution, Phys. Rep. **692**, 1 (2017).
[44] S. Nojiri and S. D. Odintsov, Unified cosmic history in modified gravity: From $F(R)$ theory to Lorentz non-invariant models, Phys. Rep. **505**, 59 (2011).
[45] B. Boisseau, G. Esposito-Farese, D. Polarski, and A. A. Starobinsky, Reconstruction of a Scalar-Tensor Theory of Gravity in an Accelerating Universe, Phys. Rev. Lett. **85**, 2236 (2000).
[46] V. Sahni and A. Starobinsky, Reconstructing dark energy, Int. J. Mod. Phys. D **15**, 2105 (2006).
[47] A. D. Dolgov, Field model with a dynamic cancellation of the cosmological constant, Pis'ma Zh. Eksp. Teor. Fiz. **41**, 280 (1985) http://www.jetpletters.ac.ru/ps/1445/article_22174.shtml.
[48] F. Bauer, J. Sola, and H. Stefancic, Dynamically avoiding fine-tuning the cosmological constant: The 'Relaxed Universe', J. Cosmol. Astropart. Phys. 12 (2010) 029.
[49] S. Y. Zhou, E. J. Copeland, and P. M. Saffin, Cosmological constraints on $f(G)$ dark energy models, J. Cosmol. Astropart. Phys. 07 (2009) 009.
[50] V. Sahni and Y. Shtanov, Braneworld models of dark energy, J. Cosmol. Astropart. Phys. 11 (2003) 014.
[51] P. Brax and C. van de Bruck, Cosmology and brane worlds: A review, Classical Quantum Gravity **20**, R201 (2003).
[52] A. Ashtekar, T. Pawlowski, and P. Singh, Quantum nature of the big bang: Improved dynamics, Phys. Rev. D **74**, 084003 (2006).
[53] A. Ashtekar and P. Singh, Loop quantum cosmology: A status report, Classical Quantum Gravity **28**, 213001 (2011).
[54] A. Chodos and S. L. Detweiler, Where has the fifth-dimension gone?, Phys. Rev. D **21**, 2167 (1980).
[55] T. Dereli and R. W. Tucker, Dynamical reduction of internal dimensions in the Early Universe, Phys. Lett. **125B**, 133 (1983).
[56] Ö. Akarsu and T. Dereli, Late time acceleration of the 3-space in a higher dimensional steady state universe in dilaton gravity, J. Cosmol. Astropart. Phys. 02 (2013) 050.
[57] J. G. Russo and P. K. Townsend, Late-time cosmic acceleration from compactification, Classical Quantum Gravity **36**, 095008 (2019).
[58] Ö. Akarsu and N. Katırcı, and S. Kumar, Cosmic acceleration in a dust only Universe via energy-momentum powered gravity, Phys. Rev. D **97**, 024011 (2018).
[59] C. V. R. Board and J. D. Barrow, Cosmological models in energy-momentum-squared gravity, Phys. Rev. D **96**, 123517 (2017).
[60] Ö. Akarsu, J. D. Barrow, C. V. R. Board, N. M. Uzun, and J. A. Vazquez, Screening Λ in a new modified gravity model, Eur. Phys. J. C **79**, 846 (2019).
[61] G. F. R. Ellis, R. Maartens, and M. A. H. MacCallum, *Relativistic Cosmology* (Cambridge University Press, Cambridge, England, 2012).
[62] G. F. R. Ellis and H. van Elst, Cosmological models: Cargèse lectures 1998, NATO Sci. Ser. C **541**, 1 (1999).
[63] M. Bouhmadi-Lopez, A. Errahmani, P. Martin-Moruno, T. Ouali, and Y. Tavakoli, The little sibling of the big rip singularity, Int. J. Mod. Phys. D **24**, 1550078 (2015).
[64] A. Bouali, I. Albarran, M. Bouhmadi-Lopez, and T. Ouali, Cosmological constraints of phantom dark energy models, Phys. Dark Universe **26**, 100391 (2019).
[65] J. D. Barrow, Graduated inflationary Universes, Phys. Lett. B **235**, 40 (1990).
[66] J. D. Barrow and K. i. Maeda, Extended inflationary universes, Nucl. Phys. **B341**, 294 (1990).
[67] J. D. Barrow and P. Saich, The behavior of intermediate inflationary universes, Phys. Lett. B **249**, 406 (1990).
[68] S. Nojiri and S. D. Odintsov, The final state and thermodynamics of dark energy universe, Phys. Rev. D **70**, 103522 (2004).
[69] H. Stefancic, Expansion around the vacuum equation of state—Sudden future singularities and asymptotic behavior, Phys. Rev. D **71**, 084024 (2005).
[70] H. Stefancic, Dark energy transition between quintessence and phantom regimes—An equation of state analysis, Phys. Rev. D **71**, 124036 (2005).
[71] P. H. Frampton, K. J. Ludwick, and R. J. Scherrer, The little rip, Phys. Rev. D **84**, 063003 (2011).
[72] J. M. Maldacena and C. Nunez, Supergravity description of field theories on curved manifolds and a no go theorem, Int. J. Mod. Phys. A **16**, 822 (2001).
[73] E. Silverstein, Simple de Sitter solutions, Phys. Rev. D **77**, 106006 (2008).
[74] U. H. Danielsson, S. S. Haque, G. Shiu, and T. Van Riet, Towards classical de Sitter solutions in string theory, J. High Energy Phys. 09 (2009) 114.
[75] T. Wrase and M. Zagermann, On classical de Sitter vacua in string theory, Fortschr. Phys. **58**, 906 (2010).
[76] U. H. Danielsson, P. Koerber, and T. Van Riet, Universal de Sitter solutions at tree-level, J. High Energy Phys. 05 (2010) 090.
[77] U. H. Danielsson, S. S. Haque, P. Koerber, G. Shiu, T. Van Riet, and T. Wrase, De Sitter hunting in a classical landscape, Fortschr. Phys. **59**, 897 (2011).
[78] X. Chen, G. Shiu, Y. Sumitomo, and S. H. H. Tye, A Global view on the search for de-Sitter vacua in (type IIA) string theory, J. High Energy Phys. 04 (2012) 026.
[79] U. H. Danielsson, G. Shiu, T. Van Riet, and T. Wrase, A note on obstinate tachyons in classical dS solutions, J. High Energy Phys. 03 (2013) 138.
[80] K. Dasgupta, R. Gwyn, E. McDonough, M. Mia, and R. Tatar, de Sitter Vacua in Type IIB string theory: Classical solutions and quantum corrections, J. High Energy Phys. 07 (2014) 054.

[81] M. Cicoli, S. De Alwis, A. Maharana, F. Muia, and F. Quevedo, De Sitter vs Quintessence in string theory, Fortschr. Phys. **67**, 1800079 (2019).
[82] C. Vafa, The string landscape and the swampland, arXiv: hep-th/0509212.
[83] U. H. Danielsson and T. Van Riet, What if string theory has no de Sitter vacua?, Int. J. Mod. Phys. D **27**, 1830007 (2018).
[84] G. Obied, H. Ooguri, L. Spodyneiko, and C. Vafa, De Sitter space and the swampland, arXiv:1806.08362.
[85] S. K. Garg and C. Krishnan, Bounds on slow roll and the de Sitter swampland, J. High Energy Phys. 11 (2019) 075.
[86] H. Ooguri, E. Palti, G. Shiu, and C. Vafa, Distance and de Sitter conjectures on the swampland, Phys. Lett. B **788**, 180 (2019).
[87] E. Palti, The swampland: Introduction and review, Fortschr. Phys. **67**, 1900037 (2019).
[88] S. Kachru, R. Kallosh, A. D. Linde, and S. P. Trivedi, De Sitter vacua in string theory, Phys. Rev. D **68**, 046005 (2003).
[89] P. Agrawal, G. Obied, P. J. Steinhardt, and C. Vafa, On the cosmological implications of the string swampland, Phys. Lett. B **784**, 271 (2018).
[90] D. Andriot, On the de Sitter swampland criterion, Phys. Lett. B **785**, 570 (2018).
[91] E. Ó Colgáin, M. H. P. M. van Putten, and H. Yavartanoo, de Sitter Swampland, H_0 tension & observation, Phys. Lett. B **793**, 126 (2019).
[92] L. Heisenberg, M. Bartelmann, R. Brandenberger, and A. Refregier, Dark energy in the swampland, Phys. Rev. D **98**, 123502 (2018).
[93] W. H. Kinney, S. Vagnozzi, and L. Visinelli, The zoo plot meets the swampland: Mutual (in)consistency of single-field inflation, string conjectures, and cosmological data, Classical Quantum Gravity **36**, 117001 (2019).
[94] Y. Akrami, R. Kallosh, A. Linde, and V. Vardanyan, The landscape, the swampland and the era of precision cosmology, Fortschr. Phys. **67**, 1800075 (2019).
[95] H. Murayama, M. Yamazaki, and T. T. Yanagida, Do we live in the swampland?, J. High Energy Phys. 12 (2018) 032.
[96] C. Han, S. Pi, and M. Sasaki, Quintessence saves Higgs instability, Phys. Lett. B **791**, 314 (2019).
[97] W. H. Kinney, Eternal Inflation and the Refined Swampland Conjecture, Phys. Rev. Lett. **122**, 081302 (2019).
[98] E. Ó Colgáin and H. Yavartanoo, Testing the swampland: H_0 tension, Phys. Lett. B **797**, 134907 (2019).
[99] J. M. Maldacena, The large N limit of superconformal field theories and supergravity, Int. J. Theor. Phys. **38**, 1113 (1999); Adv. Theor. Math. Phys. **2**, 231 (1998).
[100] E. Witten, Anti-de Sitter space and holography, Adv. Theor. Math. Phys. **2**, 253 (1998).
[101] S. A. Franchino-Viñas and S. Mignemi, Asymptotic freedom for $\lambda\phi^4_\star$ QFT in Snyder-de Sitter space, arXiv: 1911.08921.
[102] The mathematical expressions of the form x^y, when $x < 0$ and y is not an integer, should be treated carefully. The correct result of x^y is mathematically well defined without ambiguity, if it is treated with infinite numeric precision. When $x < 0$, then x^y is real valued exactly when y can be written as a fraction, m/n, where m is an integer and n is an odd integer. Furthermore, the result is positive when m is even and negative when m is odd. When y cannot be written as such, the result would be an imaginary number. Hence, to get $\rho < 0$ for $a < a_* < 1$ (or $z > z_* > 0$), we must choose $\lambda < 1$ values in accordance with these rules. The lack of continuity for λ arising from this situation would also present a practical problem for the computer models that want to raise negative numbers to fractional powers. Because computers do store fractional numbers employing finite-precision representations, the value stored in memory should always be considered a close approximation to the true value that is being represented. When a negative number is raised to a fractional power, there is no way to know whether that true value is even rational, and if it is, whether it would correspond to the positive or to the negative solution. To get around this issue when we investigate gDE computationally under the conditions given in (8), we write $\frac{\rho}{\rho_0} = x^y$ in an equivalent way as $\frac{\rho}{\rho_0} = \mathrm{sgn}(x)|x|^y$ for $y = \frac{m}{n}$ with m and n being odd integers.
[103] L. Anderson *et al.* (BOSS Collaboration), The clustering of galaxies in the SDSS-III Baryon Oscillation Spectroscopic Survey: Baryon acoustic oscillations in the data releases 10 and 11 Galaxy samples, Mon. Not. R. Astron. Soc. **441**, 24 (2014).
[104] https://github.com/slosar/april.
[105] L. E. Padilla, L. O. Tellez, L. A. Escamilla, and J. A. Vazquez, Cosmological parameter inference with Bayesian statistics, arXiv:1903.11127.
[106] A. Gómez-Valent and L. Amendola, H_0 from cosmic chronometers and Type Ia supernovae, with Gaussian processes and the novel weighted polynomial regression method, J. Cosmol. Astropart. Phys. 04 (2018) 051.
[107] S. Dodelson, *Modern Cosmology* (Academic Press, New York, 2003).
[108] D. J. Fixsen, The temperature of the cosmic microwave background, Astrophys. J. **707**, 916 (2009).
[109] W. Handley, fgivenx: A Python package for functional posterior plotting, J. Open Source Software **3**, 849 (2018).
[110] S. M. Carroll, M. Hoffman, and M. Trodden, Can the dark energy equation-of-state parameter w be less than -1? Phys. Rev. D **68**, 023509 (2003).